Journal of Orthopaedic Translation (2018) 15, 70—80

Available online at www.sciencedirect.com

ScienceDirect

journal homepage: http://ees.elsevier.com/jot

ORIGINAL ARTICLE

Magnetic resonance imaging features for the differential diagnosis of local recurrence of bone sarcoma after prosthesis replacement

Le Qin [a,☆], Qiyuan Bao [b,☆], Jie Chen [b], Lianjun Du [a], Fuhua Yan [a], Yong Lu [a], Caixia Fu [c], Weibin Zhang [b], Yuhui Shen [b,*]

[a] *Department of Radiology, Shanghai Jiao Tong University Medical School Affiliated Ruijin Hospital, No. 197 Ruijin Er Road, Shanghai 200025, China*
[b] *Department of Orthopaedics, Shanghai Jiao Tong University Medical School Affiliated Ruijin Hospital, No. 197 Ruijin Er Road, Shanghai 200025, China*
[c] *Siemens Shenzhen Magnetic Resonance Ltd, Siemens MR Center, Gaoxin C. Ave., 2nd, Hi-Tech Industrial Park, Shenzhen, China*

Received 30 May 2018; received in revised form 11 September 2018; accepted 4 October 2018
Available online 29 October 2018

KEYWORDS
Magnetic resonance imaging;
Post-operative;
Prosthesis;
Recurrence

Abstract *Objective:* To explore the imaging features of local recurrences (LRs) based on magnetic resonance imaging (MRI) after oncological orthopaedic surgery with prosthesis reconstruction.
Methods: A total of 78 cases totalling 157 scans were retrospectively reviewed. Patients with nodule/mass-like signals were retrospectively classified into LR, infectious pseudotumour, and asymptomatic pseudotumour according to clinicopathological data. LRs were histologically confirmed, and the patients without recurrences were followed up for at least 2 years. Mass size distribution and radiological characteristics were analysed for differential diagnosis of the LR versus pseudotumour.
Results: Thirty-three of 78 cases were positive with nodule/mass-like signal findings on the post-operative MRI images. By analysing the size distribution, we found that masses >2.1 cm (14) were almost attributable (98% specificity) to LRs and mostly (84.6%) timely treated. Contrarily, masses ≤2.1 cm (19) are challenging for differential diagnosis of LRs versus pseudotumour and were undertreated in five of the nine LR cases. MRI characteristics of masses ≤2.1 cm were found to be highly heterogeneous, with solid appearance, adjacent infiltration,

* Corresponding author. Department of Orthopaedics, Shanghai Jiao Tong University Medical School Affiliated Ruijin Hospital, No. 197 Ruijin Er Road, Shanghai 200025, China.
E-mail addresses: tevez10@126.com (L. Qin), rblw_110@163.com (Q. Bao), alexchen01280128@gmail.com (J. Chen), dlj10788@rjh.com.cn (L. Du), ruijin665727@qq.com (F. Yan), 18917762053@163.com (Y. Lu), caixia.fu@siemens.com (C. Fu), Zhangweibin10368@163.com (W. Zhang), yuhuiss@163.com (Y. Shen).
☆ Le Qin and Qiyuan Bao are co-first authors; they contributed equally to the work.

https://doi.org/10.1016/j.jot.2018.10.002

and less peritumour oedema being significant indicators for LRs ($P < 0.05$). Receiver operating characteristic curve showed area under curve of 0.93 for this predictive model.
Conclusions: For the post-operative MRI surveillance of oncological orthopaedic surgery with prosthesis reconstruction, a mass larger than 2.1 cm was highly specific for recurrence. When a mass was smaller than 2.1 cm, more solid property, more adjacent tissue infiltration, and less muscular oedema indicated recurrence rather than a benign mass.
The translational potential of this article: There has been very little data associated with the post-operative magnetic resonance imaging features indicating recurrence in patients with malignant bone sarcoma after prosthesis replacement. This study could help develop diagnostic features of magnetic resonance imaging for differentiating recurrence from benign changes in these patients after prosthesis replacement.

Introduction

To date, there are no universally accepted protocols for the radiological surveillance of local recurrences (LRs) after oncological prosthetic reconstruction surgery of the limb. For this reason, X-ray, computed tomography, and ultrasound used to play an important role in the detection of complications and pathologic conditions post-operatively. However, X-ray or computed tomography is less sensitive in demonstrating lesions in the deep soft tissue with potential ionising radiation hazard [1,2], while ultrasound still suffers from high degree of interoperator variability and inter-reader subjectivity [3]. Owing to its superior soft tissue contrast, magnetic resonance imaging (MRI) is theoretically a preferable modality after oncological orthopaedic surgery with prosthetic reconstruction as it is reported previously that most of the LRs occur within soft tissue rather than bone stumps for bone sarcoma such as osteosarcoma [4]. But its clinical use of imaging around prosthesis was historically limited by metal-induced artifacts. With the advent of metal artifact reduction sequence, MRI is now regaining wider popularity for post-operative follow-up with a metal implant [5—7]. Some authors have reported that optimized MRI parameters with higher bandwidth and view angle tilting (VAT) had diminished imaging metal artifact and better image quality requiring no more additional devices and scanning time compared with conventional MRI parameters [8]. A higher receiver bandwidth which attempts to orient the frequency-encoding direction along the long axis of the prosthesis can be able to decrease the voxel size, while VAT is developed to correct in-plane distortion [7,9]. These cost-effective techniques are now routinely applied in our hospital for follow-ups of patients with bone sarcoma after prosthesis replacement.

Furthermore, small size and resectability of recurrent tumours detected before resurgery are well known to be associated with better prognosis for LRs of osteosarcoma [10,11]. For this reason, accurate interpretation of post-operative radiological signs indicating LRs and complications such as pseudotumour, infection, haematoma, and scar formation in these patients contributes a lot to further management. It is noteworthy that pseudotumours are predominately reported after metal-to-metal joint arthroplasty on MRI with unclear incidence and radiological manifestations after bone tumour prosthesis placement [12—14]. The difficulty of interpreting such radiological results can be further complicated by periprosthetic imaging artifact (signal loss and distortion) and other periprosthetic abnormalities (periprosthetic effusion, oedema, and so forth.). There is no denying that the radiological differentiation between true LR versus pseudotumour condition is remarkably critical because their clinical trajectories and decision-making are drastically different. However, data regarding such issue of MRI are still lacking in the current literature. In addition, gadolinium-enhanced MRI was traditionally believed as a favourable choice for diagnosis of recurrence, but nonenhanced MRI was of low cost and more time saving which had potential to be a preferred choice for initial evaluation of suspicious patients in clinical settings.

The study objectives were to investigate whether non-enhanced MRI was feasible to detect the early signs of LRs, differentiate pathologic conditions from normal post-operative conditions, and indicate further management. To our knowledge, there were rare reports about the post-operative imaging manifestations in patients with bone malignant tumour with prosthesis by MRI [8,15].

Materials and methods

Study group and radiological evaluation

With an institutional review board approval for retrospective data analysis and a waiver of the requirement for informed consent, a cross-sectional study from January 2014 to March 2018 was conducted to examine the post-operative MRI images of patients with pathology-proven bone or soft tissue sarcoma. The inclusion criterions were the following: (1) patients who have undergone resection of the tumour segment and prosthesis replacement. All materials for prosthesis were cobalt—chromium—molybdenum alloy; (2) MRI was performed owing to clinical presentations or suspicious radiological manifestations such as abnormal oedema, swelling, and dubious mass signal from our hospital and other institutions; (3) MRI image quality met the

needs of diagnosis; (4) further management or examinations were carried out when suspecting recurrent tumours; and (5) at least 24 months of clinical follow-up in nonrecurrent patients. The exclusion criterions were the following: (1) patients were lost during the follow-up; (2) new injury to the ipsilateral limb. MRI was performed on 1.5-T Aera unit (Siemens, Erlangen, Germany) with an eight-channel body coil. High bandwidth and VAT technique were adopted to metal-induced artifacts. MRI sequences included the following: coronal T1-weighted imaging (T1WI), coronal short time inversion recovery (STIR), coronal T2-weighted imaging (T2WI), transverse T2WI, and transverse STIR. Detailed parameters of upper extremity, hip, and lower extremity were listed in Table 1–3.

For a standardized evaluation of post-operative MRI images, the following radiological features were examined: (1) nodule/mass-like signal: 0, absent; 1, present. Detailed descriptions were in the following additional evaluation; (2) muscular oedema: 0, weak or absent; 1, focal or peritumour oedema; 2, diffuse oedema. Muscular oedema was defined as regional low signal intensity on T1WI and high signal intensity on T2WI and STIR in muscle; (3) scar tissue: 0, absent; 1, present; characterized by stranded low signal intensity on all sequences; (4) lymphadenopathy: 0, absent; 1, $<$1 cm; 2, $\geq$1 cm; demonstrated as oval shaped low–intermediate signal intensity on T1WI and intermediate–high signal intensity on T2WI and STIR; (5) subcutaneous tissue oedema: 0, absent; 1, present, which was defined as patchy of diffuse low signal intensity on T1WI and high signal intensity on T2WI and STIR; (6) synovitis: 0, absent; 1, present, which was shown as massive synovial proliferation in "lamellated" or multilayered fashion within effusion, with low–intermediate signal intensity on T1WI and intermediate–high signal intensity on T2WI and STIR [16,17]; (7) periprosthesis fluid: 0, absent; 1, present; (8) osseous oedema: 0, absent; 1, present, which was demonstrated as low signal intensity on T1WI and high signal intensity on T2WI and STIR with ill-defined border on the bone structure; (9) haematoma: 0, absent; 1, present, which was demonstrated as mixed high signal intensity on T1WI and variable signal intensity on T2WI and STIR with fluid levels [18]; and (10) osteolysis: 0, absent; 1, present, which was shown as expansive and infiltrative low signal intensity on T1WI and high signal intensity on T2WI and STIR with low signal intensity rim on all sequences [19].

As mentioned previously, when the presence of nodule/mass-like signal was identified, additional parameters were also evaluated as follows: (1) cystic versus solid: 0, solid or mixed solid; 1, entirely cystic; solid mass was defined as intermediate–low signal intensity on T1WI and inhomogeneous intermediate-to-high signal intensity on T2WI and STIR [6]. Cystic mass was defined as low signal intensity on T1WI and very T2WI and STIR hyperintense signal; (2) mass count: 0, one; 1, more than one; (3) mass shape: 0, round; 1, irregular; (4) mass border: 0, well defined; 1, ill defined; and (5) adjacent tissue infiltration: 0, absent; 1, present [20,21]. Only the largest solid or cystic mass was evaluated if multiple masses existed on single MRI image.

Radiological features of all MRI images were independently evaluated by two radiologists both with more than 5 years of experience in musculoskeletal imaging who were blinded to the clinical and pathological diagnosis. When their initial description of imaging signs were dissented, a third senior radiologist with more than 10 years of experience in musculoskeletal imaging was resorted to determine the radiological signs. Their evaluation was subsequently compared with pathological and clinical results. These results were in accordance with the following rules: (1) all diagnoses of LRs were confirmed by pathological examinations; (2) diagnosis of pseudotumours was confirmed by pathological examination or radiological follow-up of minimum of 24 months; (3) infection was determined by surgery and laboratory examinations; and (4) other abnormalities were estimated by radiological follow-up of at least 24 months.

Statistical methods

Numeric data and scores were expressed as mean (range). The sensitivity and specificity curve with Youden's J statistics was used to determine the decision threshold of the tumour size in diagnosing LRs. Principal component analysis (PCA) was used to generalize the imaging features of the nodule/mass-like signal. In addition, univariate and multivariate logistic regression analyses were used to determine the significant radiological features associated with LRs. A

Table 1 Shoulder MRI sequence parameters for MRI.

Sequence/parameters	Coronal T1WI	Coronal T2WI	Coronal STIR	Transverse T2WI	Transverse STIR
TR/TE (mm)	416/13	5660/110	4060/37	5660/110	10,580/70
FoV (mm)	403	500	400	280	180
Averages	2	2	2	2	2
Slice thickness (mm)	3.0	3.0	3.0	3.0	5.0
Slices	24	28	24	40	39
Voxel size (mm)	1.3 × 1.3 × 3.0	1.3 × 1.3 × 3.0	1.3 × 1.3 × 3.0	0.7 × 0.7 × 3.0	0.6 × 0.6 × 5.0
Matrix	232 × 384	271 × 384	195 × 320	209 × 384	189 × 320
Bandwidth (Hz/Px)	334	434	391	434	434
VAT	/	50%	50%	50%	50%
Echo trains	/	15	26	10	14
Flip angle	90°	150°	150°	150°	150°

MRI = magnetic resonance imaging; TR = repetition time; TE = echo time; FoV = field of view; VAT = view angle tilting; T1WI = T1-weighted imaging; T2WI = T2-weighted imaging; STIR = short time inversion recovery.

Table 2 Hip MRI sequence parameters for MRI.

Sequence/parameters	Coronal T1WI	Coronal T2WI	Coronal STIR	Transverse T2WI	Transverse STIR
TR/TE (mm)	446/6.4	5660/110	4510/37	4660/71	9020/37
FoV (mm)	500	500	500	444	500
Averages	2	2	2	2	2
Slice thickness (mm)	3.0	3.0	3.0	4.0	4.0
Slices	24	24	24	36	30
Voxel size (mm)	1.0 × 1.0 × 3.0	1.3 × 1.3 × 3.0	1.6 × 1.6 × 3.0	0.9 × 0.9 × 4.0	1.6 × 1.6 × 4.0
Matrix	512 × 512	282 × 384	280 × 320	252 × 512	180 × 320
Bandwidth (Hz/Px)	751	434	601	610	601
VAT	50%	50%	50%	50%	50%
Echo trains	86	13	17	9	11
Flip angle	150°	150°	150°	150°	150°

TR = repetition time; TE = echo time; FoV = field of view; VAT = view angle tilting; MRI = magnetic resonance imaging; T1WI = T1-weighted imaging; T2WI = T2-weighted imaging; STIR = short time inversion recovery.

Table 3 Knee MRI sequence parameters for MRI.

Sequence/parameters	Coronal T1WI	Coronal T2WI	Coronal STIR	Transverse T2WI	Transverse STIR
TR/TE (mm)	416/13	5660/110	5660/37	5660/114	10,580/70
FoV (mm)	500	500	500	200	200
Averages	2	2	2	2	2
Slice thickness(mm)	3.0	3.0	3.0	5.0	5.0
Slices	24	24	24	25	39
Voxel size (mm)	1.3 × 1.3 × 3.0	1.3 × 1.3 × 3.0	1.6 × 1.6 × 3.0	0.5 × 0.5 × 5.0	0.6 × 0.6 × 5.0
Matrix	285 × 384	282 × 384	203 × 320	282 × 384	182 × 320
Bandwidth (Hz/Px)	334	434	391	434	434
VAT	/	50%	50%	50%	50%
Echo trains	/	13	23	13	13
Flip angle	90°	150°	150°	150°	150°

TR = repetition time; TE = echo time; FoV = field of view; VAT = view angle tilting; MRI = magnetic resonance imaging; T1WI = T1-weighted imaging; T2WI = T2-weighted imaging; STIR = short time inversion recovery.

receiver operating characteristic curve was used to evaluate this predictive model. Statistical analysis was performed using Analyse-it 4.51 and Statistical Product and Service Solutions 22.0 statistical software. *P* value of 0.05 was chosen as the threshold considered significant.

Results

Clinicopathological characteristics and MRI features

A total of 78 patients (52 males and 26 females) were included in our study with a mean age of 26.0 ± 13.8 years (7—65 years old). There were 59 osteosarcomas, including 54 conventional and five nonconventional osteosarcomas (four osteosarcomas secondary to giant-cell tumour and one osteosarcoma secondary to fibrous dysplasia), six Ewing's sarcomas, four chondrosarcomas, and seven polymorphic undifferentiated sarcomas. The remaining two cases were rhabdomyosarcoma and epithelioid angiosarcoma, which involved massive bone destruction and required prosthetic reconstruction. Affected sites included distal femur (35/78), proximal tibia (13/78), proximal femur (11/78), proximal humerus (8/78), pelvis (5/78), proximal fibula (2/78), distal humerus (2/78), distal tibia (1/78), and proximal ulna (1/78).

Among these 78 patients, nodule/mass-like signals were found in 33 patients, with 26 appearing as solid or mixed solid and seven as cystic. LRs were later proven by pathology in 22 patients (42 MR scans, with 31 scans showing masses, 18 males and four females, mean age 27.5 ± 12.5 years, range 9—52 years) with a median follow-up time of 18.6 ± 14.3 months (3—55 months) (Fig. 1A). Fifteen patients had osteosarcoma, three had Ewing's sarcoma, three had chondrosarcoma, and one had polymorphic undifferentiated sarcomas. After the initial emergence of masses on MRI, 13 patients (59.1%) underwent surgery within 1 month (mean tumour size 5.8 ± 4.3 cm, range 1.8—16 cm), seven patients (31.8%) were continually followed up by MRI showing progressing large masses and finally underwent surgery (mean tumour size of the last MRI 6.8 ± 4.9 cm, rage 2.8—16.8 cm), and for the remaining two patients (9.1%), needle biopsy was performed to confirm recurrences (tumour size 1.1 and 1.8 cm, respectively).

Of the remaining 11 pseudotumour cases (19 MRI scans), eight pseudotumours were shown to be unchanged or regressed through the course of follow-up (at least 24 months), with needle biopsy confirmed as benign reactive changes in two of them. For the other three patients, one presented with signs and symptoms suspected of infection, and two of them showed progressive manifestations of periprosthetic infection within the next month, with

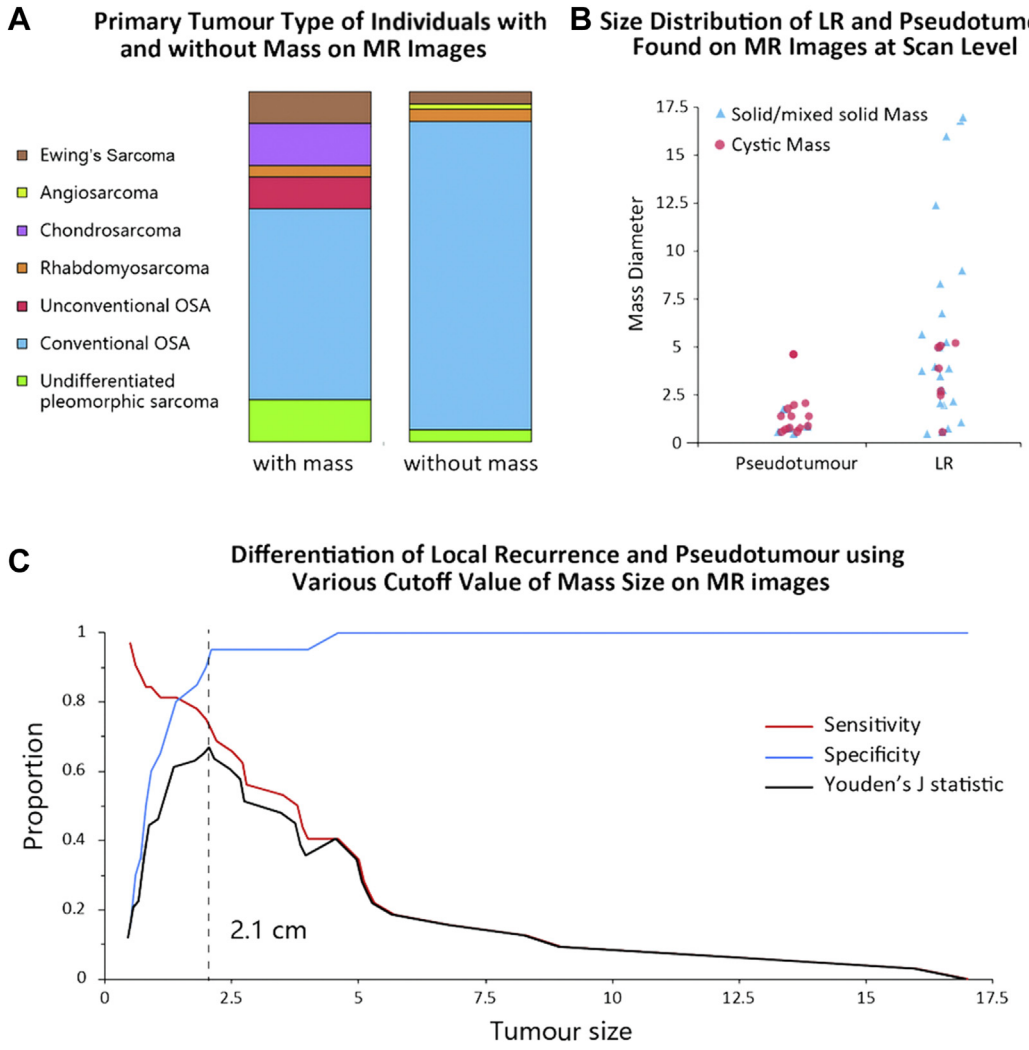

Figure 1 Size of (pseudo)tumours found on post-operative MRI images after oncological prosthetic reconstruction of extremities. (A) Pathological composition of the primary tumour undergoing MRI in our study. (B) The size distribution of solid masses and cystic mass on MRI images at the scan level. LRs mainly presented as large-sized solid or mixed solid masses, while pseudotumours, as small-sized cystic masses in appearance. (C) By comparing various cut-off values, a mass size of 2.1 cm was chosen with highest Youden's J statistics (77.4 sensitivity, 98.21% specificity), indicating that masses greater 2.1 cm on MRI images were almost attributable to LR of the malignancy. OSA = osteosarcoma; MRI = magnetic resonance imaging; LRs = local recurrences.

further evidence proving these pseudotumours as infectious origins.

Among 45 cases without nodule/mass-like signals (89 scans), muscle oedema was found in 65 images, scar tissue in 60 scans, lymphadenopathy less than 1 cm in eight scans, periprosthesis fluid in all 89 scans, osseous oedema in five images, no haematoma, synovitis in eight scans and subcutaneous oedema in 31 scans.

Differentiation of small-sized mass on MRI images

Because the large-sized mass found on the MRI image was the most intuitive diagnostic consideration of LRs, we first looked at the relationship between the mass size and mass diagnosis (Fig. 1B). Our result confirmed that LRs tended to be larger and commonly exhibited as solid appearance, while pseudotumours were smaller and mostly cystic. To reach a potential decision threshold, the sensitivity and specificity of various mass sizes for a radiological diagnosis were analysed (Fig. 1C). Youden's J statistics suggested that a cut-off value of 2.1 cm had highest diagnostic efficiency for LRs, with a limited sensitivity of 77.4 [58.9—90.4]) but a high specificity of 98.21% (95% CI 93.7—99.8%), indicating that masses greater 2.1 cm (14 cases) found on post-operative MRI images were almost attributable to LRs of the malignancy. Contrarily, a small mass not greater than 2.1 cm (19 cases) could be due to both pseudotumour (10 cases) and recurrent tumour (nine cases), thus requiring further scrutiny.

Furthermore, we retrospectively verified whether the small-sized LRs were equally treated as their big sized counterpart by the clinician during the post-operative

follow-up. In 13 patients with LRs where the initial findings of LRs were greater than 2.1 cm, 11 of 13 were further proceeded to either biopsy or surgery. Strikingly, for the remaining nine patients with LRs, only four of the nine small masses (≤2.1 cm) were timely intervened, with the rest five cases given observation for another 2–3 months, potentially missing the optimal therapeutic timing. These results suggested that the early radiological diagnosis of small LRs was challenging yet worthy of further investigation.

Heterogeneous appearance of small-sized LRs on MR images

To summarize the general features for images with small masses (≤2.1 cm) in appearance, we performed PCA to extract common patterns for LRs and pseudotumour conditions (infection and asymptomatic pseudotumours) (Fig. 2). A scree plot demonstrated that the majority (63.4%) of variance of the MRI image characteristics (excluding the periprosthesis fluid, osseous oedema and haematoma due to their extreme low variance) could be explained by the first two principal components (PCs), namely PC1 (35.5%) and PC2 (27.9%) that had the two largest possible variances. As shown in Fig. 2, the radiological appearance of LRs varied tremendously across features, with solid, infiltrative appearance with little scarring or surrounding muscular oedema as its most common manifestation (Fig. 3A and B). Our results also showed that the imaging features of LR mass with a small size could be atypical and may be misinterpreted when mimicking asymptomatic pseudotumour (Fig. 4 and Fig. 5). Infectious pseudotumours and, to a lesser extent, asymptomatic pseudotumours were clustered according to their imaging features on PCA. For example, infectious pseudotumours were typically multifocal, with synovitis at the adjacent joint and commonly occurred at the later stage (11 months, 38 months, and 65 months, in our series) (Fig. 3C and D), while asymptomatic pseudotumours commonly presented as clear-bordered, round-shaped, cystic masses (Fig. 5C and D).

Differential diagnosis of LRs for small-sized masses on MR images

To identify the radiological features differentiating LRs from pseudotumour, we performed logistic regression analysis for MRI images with ≤2.1 cm masses during post-operative follow-ups. Solid mass, adjacent infiltration, and less surrounding muscular oedema tended to be indicative of recurrent malignancies, while the opposite tended to be indicative of pseudotumour ($P < 0.05$) (Table 4). Interestingly, the predictive model using such three variables yielded an area under curve (AUC) of 0.93 as shown by receiver operating characteristic curve analysis (Fig. 6).

Next, for MRI images with small-sized recurrent tumours (≤2.1 cm), we asked whether other accompanying positive findings such as scar, subcutaneous oedema, mass border, muscular oedema, lymphadenopathy, mass shape, synovitis, mass count, haematoma, osseous oedema, osteolysis, periprosthetic fluid, and so forth might differ from the normal post-operative control, thus raising diagnostic

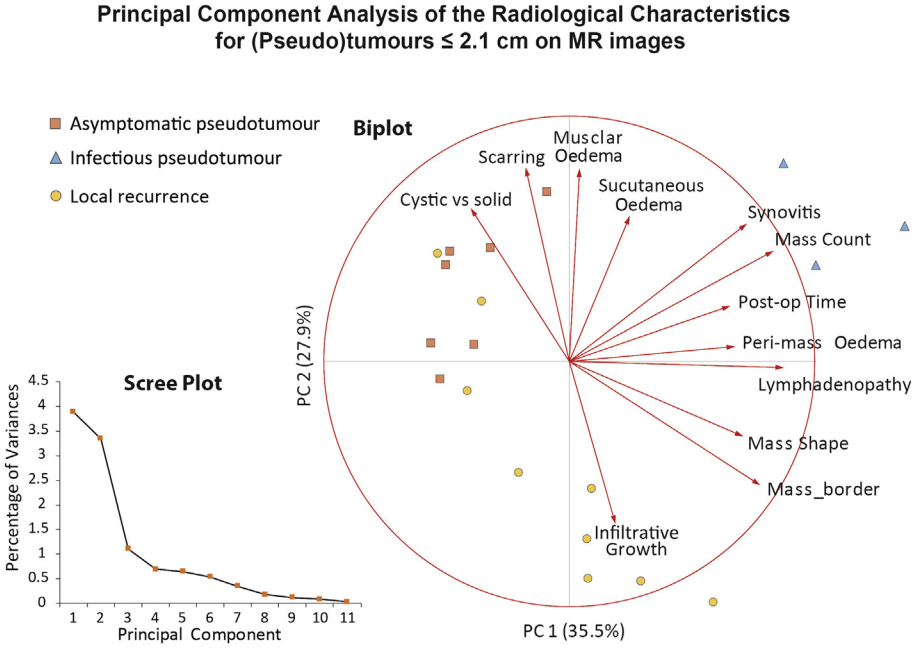

Figure 2 Principal component analysis of the radiological characteristics of LRs and pseudotumours on post-operative MRI images. The scree plot suggests that the majority (63.4%) of variance could be explained by PC1 (35.5%) and PC2 (27.9%). As indicated by the biplot, infectious pseudotumours and asymptomatic pseudotumours were clustered according to their imaging features on PCA. However, the radiological characteristics of LRs varied tremendously, with solid, infiltrative appearance with little scarring or surrounding oedema as its most common type.
PCA = principal component analysis; MRI = magnetic resonance imaging; LRs = local recurrences.

Figure 3 Typical signs of recurrent tumours and infection on MRI images. (A) Local recurrence (arrowhead) of osteosarcoma in the right proximal femur was found anterior to the femur prosthesis (upper). On transverse T2WI image, the mass was presented as intermediate-to-high signal intensity with infiltration to the adjacent muscle and fat tissue. The malignancy was resistant to chemotherapy and progressively invaded into the adjacent tissue (lower). (B) A small-sized mass in the left humerus was detected close to the distal humerus prosthesis. Coronal T2WI image showed a solid mass in intimate relation with adjacent muscle without obvious peritumour oedema. Re-resection of the lesion proved it to be recurrent Ewing's sarcoma. (C, D) A 22-year-old male complained of mild knee pain 38 months after osteosarcoma resection and prosthetic reconstruction in the left distal femur. Coronal T2WI MRI showed cystic masses (arrowhead) accompanied by "lamellated" synovitis, which was later diagnosed to be periprosthetic infection.
MRI = magnetic resonance imaging; T2WI = T2-weighted imaging.

performance of LRs. However, our results suggested that none of these MRI findings were significant indicators associated with LRs ($P > 0.05$, some detailed data were not shown).

Discussion

The most significant findings of our study were that for routine follow-ups in patients with bone sarcomas after prosthesis surgery, MRI could also detect tumours, demonstrate the early signs of LRs, and identify benign lesions.

Because small size and resectability of recurrent tumours were reported to be favourable prognostic factors for bone malignancies such as osteosarcoma, promptly identifying recurrent malignancies could not only increase the limb salvage rate but also potentially improve overall patient survival [10,11]. Consistent with the previous reports, we have observed a high incidence of pseudotumour (11 of 78) on MRI images, which demanded further endeavours to make differential diagnosis [22,23]. Our study found some useful signs and manifestations to evaluate post-operative noncontrast MRI images in these patients to help orthopaedists to decide the next step, which consist of routine follow-up, further examination, alteration of chemotherapy treatment, needle biopsy, and surgery.

In our analysis, we found that the mass displayed on the MRI image, whenever its size exceeded 2.1 cm, should prompt responsible clinicians to consider tumour recurrence. Besides, for the early detected small mass on MRI that is not greater than 2.1 cm, three characteristics are significant for the radiological differential diagnosis of LRs. One is the presence of localized intermediate-to-high T2WI or STIR signal intensity, representing solid or mixed solid

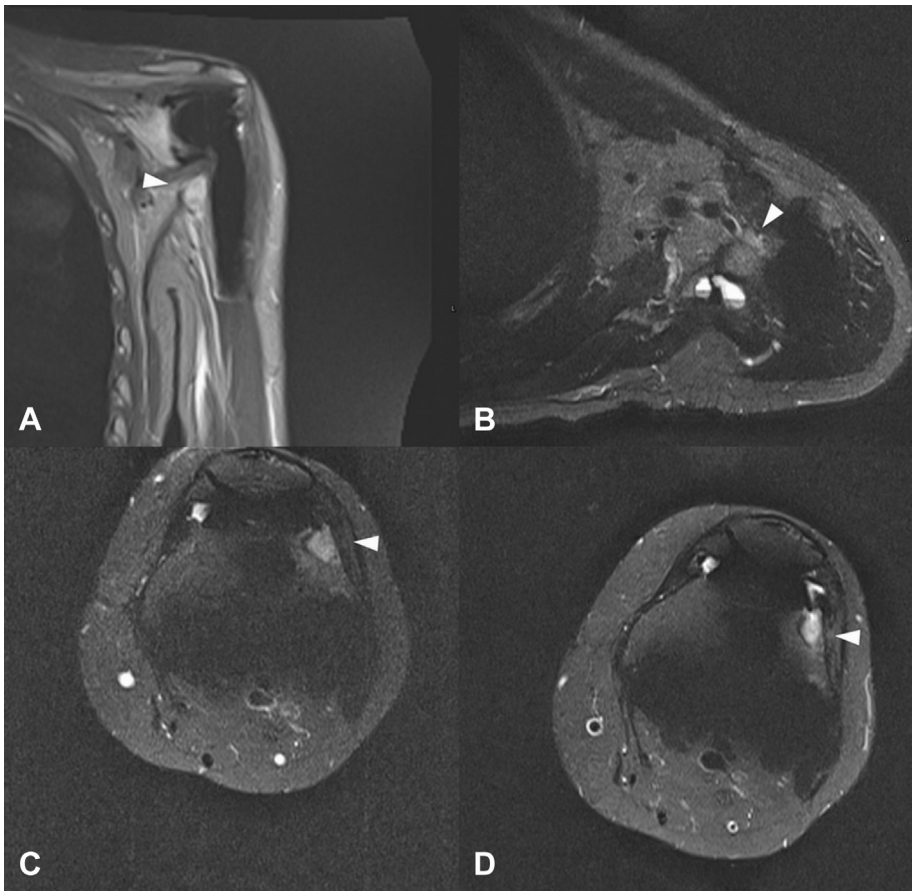

Figure 4 Solid pseudotumour mimicking local recurrence. A small-sized recurrent osteosarcoma in the left proximal humerus was shown on coronal T2WI (A) and transverse STIR (B) MRI images, as an infiltrative mixed solid mass (arrowhead). Haematoma was seen posterior to the mass. (C, D): A 42-year-old female underwent tumour resection on the left distal femur, with pathological diagnosis of osteosarcoma secondary to fibrous dysplasia. At 6 months post-operatively, transverse STIR MRI (C) demonstrated a solid, irregular-shaped mass of 6 mm in diameter on the distal femur lateral to prosthesis. The mass was very similar to an early detected small-sized LR of osteosarcoma, despite a lesser extent of peritumour infiltration. However, it slightly regressed and remained asymptomatic during the next 2 years, thus being considered pseudotumour (D).
T2WI = T2-weighted imaging; STIR = short time inversion recovery; MRI = magnetic resonance imaging; LR = local recurrence.

masses in the muscle and adipose space. In our study, solid or mixed solid masses were found in all except one patient with LRs, while six of 11 pseudotumours are cystic. This result was in parallel with the previous literature, suggesting solid pseudotumours were uncommon [24]. The other two features are adjacent tissue infiltration and less surrounding muscular oedema. In other words, a small LR tends to appear invasive, but with little muscular oedema probably because its size is too limited to evoke extensive muscular oedema. However, our PCA analysis demonstrated that the MRI appearance of LRs was more heterogeneous than that of benign pseudotumour, indicating the difficulty of generalising all LRs into a stereotypical pattern. In our opinion, whenever an ambiguously appearing mass with any one of these features is seen during the MRI follow-up, awareness should be raised, and further examinations such as enhanced MRI and other modalities might be needed before definitive diagnosis.

Noninfectious pseudotumour has been associated with aseptic inflammation, or necrotic tissue, and could sometimes be progressive according to literature [25]. However, in our study, the only three progressive pseudotumours were associated with infectious origin, with the same incidence as the previous report by Aponte-Tinao et al. (5.7%) [26]. We felt that critical clues to infection included extensive deep soft tissue swelling, sinus tract, considerable synovitis, and accompanied small solid masses representing abscesses. The more the signs appear, the higher the likelihood of infection is. Synovitis could appear as either "lamellated" or multilayered fashion, which has been proved to be, especially, a high sensitive and specific sign for diagnosing infection [17].

For the remaining eight asymptomatic pseudotumours, our data suggested that these masses were nonprogressive and required no specific intervention, at least within the afterward 2 years. Recent studies have demonstrated that pseudotumors were frequent findings without associations with the prosthesis position and wear [27]. In patients who underwent total hip arthroplasties, cystic lesions around prosthesis, accounting for most pseudotumours, were

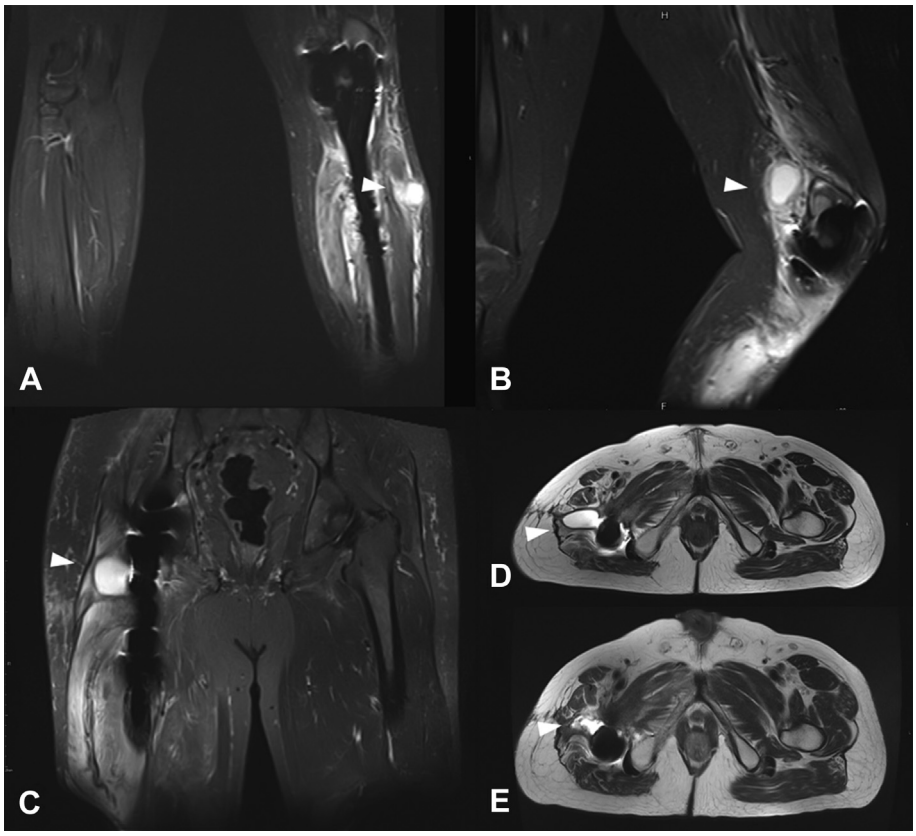

Figure 5 Cystic local recurrent tumour mimicking pseudotumour. (A) A progressively enlarged mass was found in the left proximal tibia with a history of conventional osteosarcoma. A coronal STIR MRI image demonstrated a cystic mass (arrowhead) of 1.7 cm lateral to proximal prosthesis. Note its slightly more ill-defined edge towards adjacent muscle with weak muscular oedema. The mass was subsequently resected, with pathology being be a recurrent malignancy. Interestingly, (B) showed that another local recurrent mass reappeared at another proximal site with very similar appearance to the recurrence in (A) 2 months after the second surgery. A cystic asymptomatic pseudotumour in another osteosarcoma patient was shown in (C) and (D). This pseudotumour was highly similar to (A) and (B), except that it was communicated with a joint cavity. After 6 months, cystic pseudotumour was shown to be regressed with an irregular contour (arrowhead) (E).
STIR = short time inversion recovery; MRI = magnetic resonance imaging.

Table 4 Radiological features on MR imaging for nodular/mass-like signal ≤2.1 cm.

Radiological feature	Classification	Pseudotumours	LR	*P* value	*b* value	Odds ratio	Confidence interval
Peritumour oedema	Absent	5	6	0.01*	−0.48	0.62	0.41 ~ 0.94
	Present	5	3				
Cystic vs solid	(mixed) solid	3	8	0.03*	−0.44	0.64	0.44 ~ 0.95
	Cystic	7	1				
Infiltration	Absent	10	6	0.01*	0.74	2.09	1.13 ~ 3.84
	present	0	3				

MR = magnetic resonance; LR = local recurrence.
Continuous variables are described as median (range)
*Significant in multivariate logistic model with backward selection method.

normal findings without significant correlation to poor clinical results [24,28]. But solid lesions could bring out relevant clinical symptoms. Cystic lesions might relate to sterile inflammation, while solid lesions mainly to necrotic tissue [25]. In our study, nonprogressive pseudotumours also occupied a large proportion of pseudotumours, which were composed of cystic and solid masses. Similarly, none of them was associated with recurrence and revision surgery.

Periprosthesis fluid and muscle oedema were also commonly normal changes in prosthesis surgery. Periprosthesis fluid was found in almost all of our patients, and we do not consider it as a meaningful indicator for recurrence. Sabah et al. found muscle oedema in eight patients with metal-on-metal hips, but they did not analysis the reason for these conditions [25]. We felt that such conditions might be related to muscular reaction to prosthesis and surgery trauma.

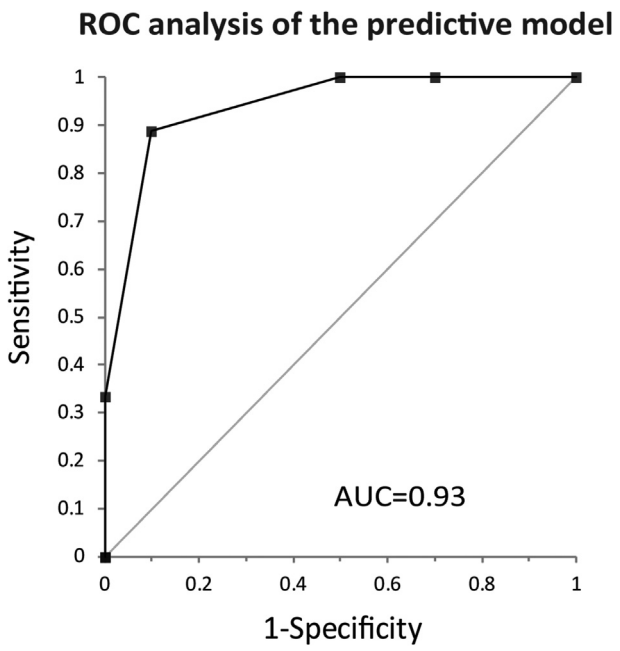

Figure 6 ROC for the predictive model. AUC of this ROC was 0.93, indicating high diagnostic accuracy for the predictive model of three significant variables. ROC, receiver operating characteristic curve; AUC, area under curve.

We acknowledged some limitations in our study. First, enhanced MRI has not been performed in the majority of our patients. Although it has been reported that static enhanced MRI obtained 2—5 min after contrast medium injection was not always able to differentiate between tumour recurrence and benign changes, dynamic contrast-enhanced (DCE) MRI was considered to be very helpful owing to the unique pattern of fast enhancement of recurrence [29,30]. However, it was uncertain whether DCE MRI was available in patients after prosthesis replacement because of the influence of metal artifacts. According to our results, large masses and certain typical malignant manifestation of small masses less than 2.1 cm could avoid some unnecessary enhanced examinations. So DCE MRI should be optimized in terms of image quality and applied in some unequivocal masses to detect LRs in postsurgical follow-up in the future. Second, the sample size was relatively small, and patients included were mainly performed by MRI because of suspicious clinical and radiological manifestations, which would lead to some extent of selection bias. That was why the recurrent rate in our study was relatively high. Future studies should include all patients who performed routine MRI postoperatively. Finally, lacking long-term follow-up did not allow us to know about MRI signs of long-term recurrence and complications.

Conclusion

In conclusion, for patients with prosthesis, we could detect the recurrence and diverse benign complications or conditions based on post-operative MRI. A mass larger than 2.1 cm was highly specificity for recurrence. When a mass was smaller than 2.1 cm, more solid property, more adjacent tissue infiltration, and less muscular oedema indicated recurrence rather than a benign mass.

Funding

This study was supported by funding of Science and Technology Committee of Shanghai (grant numbers 17411964900).

Conflict of Interest Statement

The authors declare that they have no conflict of interest.

References

[1] Talbot BS, Weinberg EP. MR Imaging with metal-suppression sequences for evaluation of total joint arthroplasty. Radiographics 2016;36:209—25.
[2] Robinson E, Henckel J, Sabah S, Satchithananda K, Skinner J, Hart A. Cross-sectional imaging of metal-on-metal hip arthroplasties. Can we substitute MARS MRI with CT? Acta Orthop 2014;85:577—84.
[3] Kwon YM, Dimitriou D, Liow MH, Tsai TY, Li G. Is ultrasound as useful as metal artifact reduction sequence magnetic resonance imaging in longitudinal surveillance of metal-on-metal hip arthroplasty patients? J Arthroplasty 2016;31:1821—7.
[4] Jeon DG, Song WS, Kong CB, Cho WH, Cho SH, Lee JD, et al. Role of surgical margin on local recurrence in high risk extremity osteosarcoma A case-controlled study. Clin Orthop Surg 2013;5:216—24.
[5] Agten CA, Del Grande F, Fucentese SF, Blatter S, Pfirrmann CW, Sutter R. Unicompartmental knee arthroplasty MRI: impact of slice-encoding for metal artefact correction MRI on image quality, findings and therapy decision. Eur Radiol 2015;25:2184—93.
[6] Bermejo A, De Bustamante TD, Martinez A, Carrera R, Zabia E, Manjon P. MR imaging in the evaluation of cystic-appearing soft-tissue masses of the extremities. Radiographics 2013;33:833—55.
[7] Chen CA, Chen W, Goodman SB, Hargreaves BA, Koch KM, Lu W, et al. New MR imaging methods for metallic implants in the knee: artifact correction and clinical impact. J Magn Reson Imag 2011;33:1121—7.
[8] Jiang MH, He C, Feng JM, Li ZH, Chen Z, Yan FH, et al. Magnetic resonance imaging parameter optimizations for diagnosis of periprosthetic infection and tumor recurrence in artificial joint replacement patients. Sci Rep 2016;6:36995.
[9] Gutierrez LB, Do BH, Gold GE, Hargreaves BA, Koch KM, Worters PW, et al. MR imaging near metallic implants using MAVRIC SL: initial clinical experience at 3T. Acad Radiol 2015;22:370—9.
[10] Rodriguez-Galindo C, Shah N, McCarville MB, Billups CA, Neel MN, Rao BN, et al. Outcome after local recurrence of osteosarcoma: the St. Jude Children's Research Hospital experience (1970-2000). Cancer 2004;100:1928—35.
[11] Grimer RJ, Sommerville S, Warnock D, Carter S, Tillman R, Abudu A, et al. Management and outcome after local recurrence of osteosarcoma. Eur J Canc 2005;41:578—83.
[12] Kwon YM, Liow MH, Dimitriou D, Tsai TY, Freiberg AA, Rubash HE. What is the natural history of "asymptomatic" pseudotumours in metal-on-metal hip arthroplasty? Minimum 4-year metal artifact reduction sequence magnetic resonance imaging longitudinal study. J Arthroplasty 2016;31:121—6.
[13] Lindgren K, Anderson MB, Peters CL, Pelt CE, Gililland JM. The prevalence of positive findings on metal artifact reduction

sequence magnetic resonance imaging in metal-on-metal total hip arthroplasty. J Arthroplasty 2016;31:1519—23.
[14] van der Weegen W, Smolders JM, Sijbesma T, Hoekstra HJ, Brakel K, van Susante JL. High incidence of pseudotumours after hip resurfacing even in low risk patients; results from an intensified MRI screening protocol. Hip Int 2013;23:243—9.
[15] Susa M, Oguro S, Kikuta K, Nishimoto K, Horiuchi K, Jinzaki M, et al. Novel MR imaging method-MAVRIC-for metal artifact suppression after joint replacement in musculoskeletal tumor patients. BMC Muscoskel Disord 2015;16:377.
[16] Prasad A, Manchanda S, Sachdev N, Baruah BP, Manchanda V. Imaging features of pediatric musculoskeletal tuberculosis. Pediatr Radiol 2012;42:1235—49.
[17] Sneag DB, Bogner EA, Potter HG. Magnetic resonance imaging evaluation of the painful total knee arthroplasty. Semin Muscoskel Radiol 2015;19:40—8.
[18] Yarmish G, Klein MJ, Landa J, Lefkowitz RA, Sinchun H. Imaging characteristics of primary osteosarcoma nonconventional subtypes. Radiographics 2010;30:1653—72.
[19] Hayter CL, Potter HG, Su EP. Imaging of metal-on-metal hip resurfacing. Orthop Clin N Am 2011;42:195—205.
[20] Errani C, Kreshak J, Ruggieri P, Alberghini M, Picci P, Vanel D. Imaging of bone tumors for the musculoskeletal oncologic surgeon. Eur J Radiol 2013;82:2083—91.
[21] Miller BJ, Avedian RS, Rajani R, Leddy L, White JR, Cummings J, et al. What is the use of imaging before referral to an orthopaedic oncologist A prospective, multicenter investigation. Clin Orthop Relat Res 2015;473:868—74.
[22] Ferrari S, Balladelli A, Palmerini E, Vanel D. Imaging in bone sarcomas. The chemotherapist's point of view. Eur J Radiol 2013;82:2076—82.
[23] Loh AH, Navid F, Wang C, Bahrami A, Wu J, Neel MD, et al. Management of local recurrence of pediatric osteosarcoma following limb-sparing surgery. Ann Surg Oncol 2014;21:1948—55.
[24] Fehring TK, Odum S, Sproul R, Weathersbee J. High frequency of adverse local tissue reactions in asymptomatic patients with metal-on-metal THA. Clin Orthop Relat Res 2014;472:517—22.
[25] Sabah SA, Mitchell AW, Henckel J, Sandison A, Skinner JA, Hart AJ. Magnetic resonance imaging findings in painful metal-on-metal hips: a prospective study. J Arthroplasty 2011;26:71—6. 6 e1-2.
[26] Aponte-Tinao L, Ayerza MA, Muscolo DL, Farfalli GL. Survival, recurrence, and function after epiphyseal preservation and allograft reconstruction in osteosarcoma of the knee. Clin Orthop Relat Res 2015;473:1789—96.
[27] Matthies AK, Skinner JA, Osmani H, Henckel J, Hart AJ. Pseudotumors are common in well-positioned low-wearing metal-on-metal hips. Clin Orthop Relat Res 2012;470:1895—906.
[28] Bisseling P, de Wit BW, Hol AM, van Gorp MJ, van Kampen A, van Susante JL. Similar incidence of periprosthetic fluid collections after ceramic-on-polyethylene total hip arthroplasties and metal-on-metal resurfacing arthroplasties: results of a screening metal artefact reduction sequence-MRI study. Bone Joint Lett J 2015;97-B:1175—82.
[29] Shapeero LG, De Visschere PJ, Verstraete KL, Poffyn B, Forsyth R, Sys G, et al. Post-treatment complications of soft tissue tumours. Eur J Radiol 2009;69:209—21.
[30] Verstraete KL, Lang P. Bone and soft tissue tumors the role of contrast agents for MR imaging. Eur J Radiol 2000;34:229—46.